Accepted Manuscript

Electrochemical Biosensor for Methyl Parathion Based on Single-Walled Carbon Nanotube/Glutaraldehyde Crosslinked Acetylcholinesterase-Wrapped Bovine Serum Albumin Nanocomposites

T.H. Vignesh Kumar, Ashok K. Sundramoorthy

PII: S0003-2670(19)30555-0

DOI: https://doi.org/10.1016/j.aca.2019.05.011

Reference: ACA 236774

To appear in: *Analytica Chimica Acta*

Received Date: 18 January 2019

Revised Date: 19 April 2019

Accepted Date: 5 May 2019

Please cite this article as: T.H.V. Kumar, A.K. Sundramoorthy, Electrochemical Biosensor for Methyl Parathion Based on Single-Walled Carbon Nanotube/Glutaraldehyde Crosslinked Acetylcholinesterase-Wrapped Bovine Serum Albumin Nanocomposites, *Analytica Chimica Acta*, https://doi.org/10.1016/j.aca.2019.05.011.

This is a PDF file of an unedited manuscript that has been accepted for publication. As a service to our customers we are providing this early version of the manuscript. The manuscript will undergo copyediting, typesetting, and review of the resulting proof before it is published in its final form. Please note that during the production process errors may be discovered which could affect the content, and all legal disclaimers that apply to the journal pertain.

GRAPHICAL ABSTRACT:

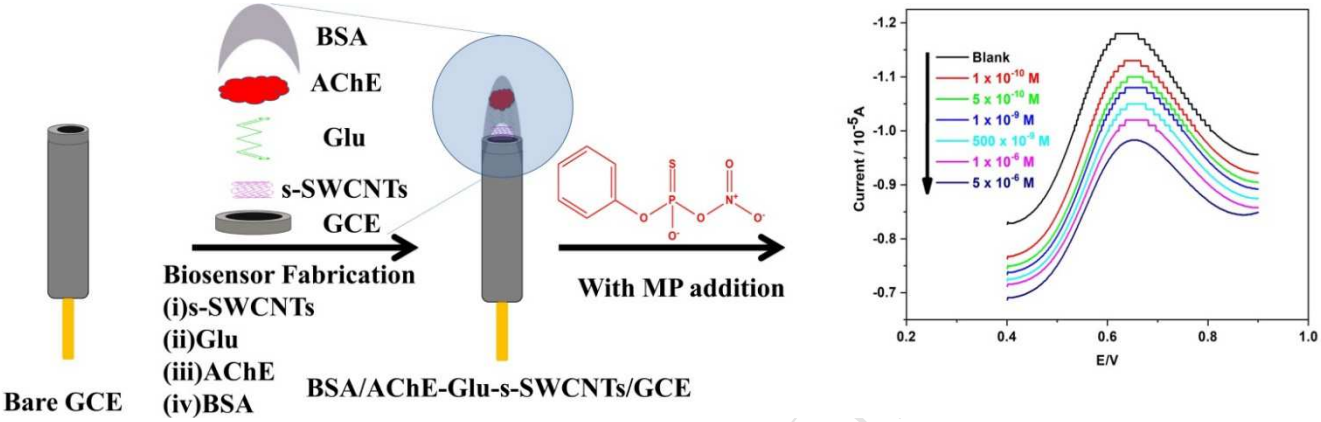

ACCEPTED MANUSCRIPT

ACCEPTED MANUSCRIPT

Electrochemical Biosensor for Methyl Parathion Based on Single-Walled Carbon Nanotube/Glutaraldehyde Crosslinked Acetylcholinesterase-Wrapped Bovine Serum Albumin Nanocomposites

T.H. Vignesh Kumar[1] and Ashok K. Sundramoorthy[1,*]

[1]Department of Chemistry, SRM Institute of Science and Technology, Kattankulathur

603203, Tamil Nadu, India

ACCEPTED MANUSCRIPT

*Corresponding author:
Ph.: +91-44-27417686
Email: ashokkumar.sun@ktr.srmuniv.ac.in

ABSTRACT

Semiconducting single-walled carbon nanotubes (s-SWCNTs) have demonstrated as excellent material for transistors, miniaturized devices and sensors due to their high carrier mobility, stability, scattering-free ballistic transport of carriers *etc*. Herein, we have designed a biosensor to selectively detect methyl parathion (MP, organophosphorus pesticide) using glutaraldehyde (Glu) cross-linked with acetylcholinesterase (AChE) immobilized on s-SWCNTs wrapped with bovine serum albumin (BSA). The fabricated biosensor was characterized and confirmed by Fourier-transform infrared spectroscopy (FT-IR), cyclic voltammetry (CV), electrochemical impedance spectroscopy (EIS) and square wave voltammetry (SWV). In the presence of MP, the effective interaction between AChE and MP favours the accumulation of MP-AChE complex on the glassy carbon electrode (GCE) surface which reduces the electron transfer property. Based on this interaction, detection of various concentration of MP was demonstrated by SWV using BSA/AChE-Glu-s-SWCNTs composite modified electrode. The proposed biosensor exhibited a wide linear range (WLR) for MP target in 100 mM phosphate buffered saline solution (PBS) (pH 7.4) from 1×10^{-10} M to 5×10^{-6} M with a limit of detection (LOD) of 3.75×10^{-11} M. In addition, the BSA/AChE-Glu-s-SWCNTs/GCE biosensor showed good repeatability and reproducibility for MP detection. Moreover, the proposed biosensor showed better electrode stability when stored at 4°C. This new electrochemical biosensor is also exhibited high selectivity and sensitivity for MP, which made it possible to test MP in real strawberry and apple juices. Furthermore, the BSA/AChE-Glu-s-SWCNTs/GCE offered a favourable electron transfer between the target MP and electrode interface than BSA/AChE-s-SWCNTs/GCE, s-SWCNTs/GCE and bare GCE.

***Keywords*:** Semiconducting SWCNTs; Biosensor; Methyl parathion detection; Real sample analysis.

1. INTRODUCTION

ACCEPTED MANUSCRIPT

Organophosphorus pesticides (i.e. methyl parathion (MP), chlorpyrifos, diazinon, dichlorvos, phosmet, fenitrothion, tetrachlorvinphos, azamethiphos, azinphos-methyl and terbufos) are widely used to protect the agricultural crops (For examples: wheat, rice plants, vegetables and fruits) from insect damages. The residues of utilized organophosphorus pesticide may enter in to the food chain through agricultural crops, water, soil and air [1–4]. Pesticides are highly toxic and act as inhibitors of the cholinesterase enzyme in the human and animal bodies which will cause Peripheral neuropathy (PN). The PN is a damage to different nerves in the human and animals, which may impair movement, sensation, gland secretion or organ function and other health issues depends on their type of nerves affected [5,6]. It was estimated that world-wide one million people per year get affected by chronic diseases and deaths from pesticide contaminated foods [7]. In this context, Food Quality Protection Act (FQPA) directed United States Environmental Protection Agency (US-EPA) to completely re-evaluate pesticide contaminations in food [8]. Therefore, US-EPA used the improved food safety standards in FQPA to ban the use of 270 pesticides (i.e. including methyl parathion) for food and household purposes [8]. Nevertheless, MP has been widely used in agricultural fields. So, US-EPA strictly monitors the food contamination from MP residues [9]. MP was commonly monitored or detected by routine methods such as colorimetry [10], mass spectrometry [11], liquid/gas chromatography [12], Raman [13] and photoluminescence/fluorescence spectroscopies [14,15]. However, electrochemical biosensors have been demonstrated with several advantages such as fast analysis, high sensitivity and selectivity, no interference effect, real-time analysis and relatively low cost [16–22].

Single-walled carbon nanotubes (SWCNTs) are highly recognized as good electrode materials to fabricate electrochemical sensors because of many analytes can be detected at lower potential with high sensitivity and selectivity in real sample matrix [16,23–27]. But,

ACCEPTED MANUSCRIPT

during synthesis of SWCNTs, mixture of nanotubes was obtained with different metallicity, chirality, length and diameter. It was reported that these polydispersity of nanotubes might affect the conductivity of the SWCNTs film and also complete removal of metallic SWCNTs is necessary to fabricate switchable biosensing field effect transistors (FETs) using semiconducting SWCNTs (s-SWCNTs) [28–30]. Likely, the metallic nanotubes could easily short the device, so it cannot be used in FETs [31–33]. The s-SWCNTs are ideal transducers along with the integration of biomolecules as an adequate way of developing electrochemical biosensors which allows us to fabricate FETs [34–36]. In particular, s-SWCNTs have been demonstrated in a high performance FETs and integrated circuits utilizing the aligned nanotubes on different kinds of flexible and rigid substrates [31]. Thereby, s-SWCNTs have accelerated tremendous interest in both fundamental and practical research in nano, micro and macro electronic based sensors [31]. In this context, s-SWCNTs based FETs as a biosensor platform for pesticide detection is investigated. To the best of author's knowledge, there has been no reports on the s-SWCNTs based electrochemical biosensor for pesticide detection.

Recently, Oh *et al.* developed an electrochemically modulated SWCNTs network based flexible sensor for determination of dopamine from 1.5 to 30 µM in the presence of 100 µM ascorbic acid and 10 µM uric acid in 0.1 M PBS (pH 7.4) [33]. After electrochemical oxidation, resistance of SWCNTs network electrode was reduced by 52%. As we know that a typical SWCNT network contains both s-SWCNTs and metallic-SWCNTs (2:1 ratio) [33]. The co-existence of semiconducting and metallic nanotubes could form a Schottky barrier junction, which greatly suppresses the charge flow. The electrochemical oxidation of SWCNTs network is likely attributed to suppressing of Schottky barrier [33,37]. In addition, electrochemical oxidation process can generate oxygen containing functional groups such as hydroxyl, carbonyl and carboxylate on SWCNTs network electrode with electrocatalytic activity [33]. Kiani *et al.* designed SWCNTs based ion sensitive FET device for pH detection

ACCEPTED MANUSCRIPT

[38]. The sensing mechanism was explained based on the interaction between SWCNTs and ionic solution (with different pH) which caused considerable alterations of π electrons on nanotube network by electrostatic gating method [38]. In this direction, extensive research works have been conducted to develop the wearable sensors with ultrathin thickness and stretchability [39]. Graphene is a zero band gap material with low on/off ratio and cannot be effectively utilized to fabricate switchable FETs with high on/off ratio [40]. As a potential candidate, s-SWCNTs are very attractive and promising material for digital circuits due to their intrinsically high carrier mobility. However, still there are some challenges remain to get high purity s-SWCNTs by separation process, device fabrication, material optimization strategies *etc.* [39,40]. In order to get high performance devices, s-SWCNTs based electronic device components are required for next generation advanced biosensors [29,41,42].

On the other hand, excess usage of pesticides resulted in discharge of pesticides and their photochemical transformation leads to their metabolites in the environments. This serious problem made us to develop new biosensors which can accurately detect or identify pesticides and their metabolites in food and environmental samples [43]. The acetylcholinesterase (AChE) enzyme-based biosensor is a versatile method for the determination of organophosphate and carbamate-based pesticides due to the natural inhibition of enzymes by the usage of the target analyte [44–48]. AChE could undergo hydrolysis with acetylthiocholine chloride (ATCl) to produce thiocholine (Tch) which is a useful medium for pesticide detection [48]. The sensing mechanism is based on AChE inhibition due to blocking the serine hydroxyl group by covalently bound phosphorous atom of organophosphates and carbonyl carbon of carbamates [44,48,49].

Many cross-linkers (i.e. N-hydroxysuccinimide, 1-ethyl–3-3 dimethylaminopropyl carbodiimide hydrochloride, epichlorohydrin glyoxal and Glutaraldehyde (Glu)) were used to design the novel bioelectronic devices for highly stable and selective target detection [48,50]. For instance, Viswanathan *et al*. proposed the Glu cross-linked AChE immobilized

ACCEPTED MANUSCRIPT

polyaniline deposited SWCNTs wrapped single strand oligonucleotide on the gold electrode for MP and chlorpyrifos detection [48]. However, AChE enzyme based biosensors are easily affected by acetic acid during electrochemical oxidation of acetylthiocholine [48,51]. Hence, the good selective nature of MP sensor can be attributed to the excellent inhibition of acetylthiocholine and combination effect of BSA coating which are facilitating the electron transfer process from electrolyte to electrode surface and also eliminated the interferent molecules [51].

In this work, we have fabricated a simple and effective electrochemical biosensor for MP detection in fruits by using high purity s-SWCNTs modified electrode. The Glu is effectively cross-linked with AChE and s-SWCNTs. It was confirmed by FT-IR, CV, EIS and SWV techniques. As prepared, BSA/AChE-Glu-s-SWCNTs/GCE biosensor was used to detect MP in the range from 1×10^{-10} M to 5×10^{-6} M with a detection limit of 3.75×10^{-11} M. Effects of interferent were studied with glucose (GU), uric acid (UA), oxalic acid (OA), ascorbic acid (AA) and orthophosphoric acid (OPA). Moreover, detection of MP was demonstrated in apple and strawberry juices using a BSA/AChE-Glu-s-SWCNTs composite modified electrode in phosphate buffered saline (PBS).

2. EXPERIMENTAL

2.1. Chemicals and reagents

AChE from electrophorus electricus (electric eel) (C3389-2KU), ATCl (purity ≥99%), TLC powder (A5626-1G), 3-aminopropyl triethoxysilane (APTES), bovine serum albumin (BSA) and MP were purchased from Sigma-Aldrich (St. Louis and New Haven, USA). Glutaraldehyde (Glu) 25% in water (CAS 111-30-8) was purchased from Spectrochem Pvt. Ltd. (Mumbai, India). Separated semiconducting single-walled carbon nanotubes (s-SWCNTs) dispersion was received from the laboratory of Prof. M.B. Chan-Park [52]. All other chemicals and reagents used in this study were of analytical grade. The electrolyte

ACCEPTED MANUSCRIPT

solution was 100 mM PBS (pH 7.4) which was prepared by using potassium monohydrogen phosphate (K_2HPO_4) and potassium dihydrogen phosphate (KH_2PO_4) in an aqueous medium. All aqueous solutions were freshly prepared by Milli-Q water (18.2 MΩ cm^{-1}, specific resistivity) collected from Millipore Water System.

2.2. Instruments

2.2.1. Spectroscopy and microscopy studies

The s-SWCNTs were characterized using a Varian Cary 4000 ultraviolet-visible-near infrared (UV-vis-NIR) spectrophotometer and Renishaw Raman microscope equipped with 514 nm wavelength (2.41 eV) laser source in a backscattering configuration. Transmission electron microscopy (TEM) analysis was done with (JEM-2100 plus, Jeol) operating at 200 kV. Attenuated total reflection Fourier-transform infrared spectroscopy (FT-IR) was recorded on a Bruker α-E (Lab India Instruments Private Limited, Mumbai).

2.2.2. Electrochemical studies

Electrochemical impedance spectroscopy (EIS), cyclic voltammetry (CV) and square wave voltammetry (SWV) measurements were carried out using electrochemical workstation CHI-760E (CH Instruments, Inc. Austin, USA). Glassy carbon electrode (3 mm diameter) (GCE), platinum wire and Ag/AgCl (1 M KCl) were used as working, counter and reference electrodes, respectively (purchased from CH Instruments, Inc. Austin, USA). EIS was performed in 0.1 M KCl containing 5 mM $K_3[Fe(CN)_6]$ and 5 mM $K_4[Fe(CN)_6]$ by applying different frequency of AC impedance from 10 Hz to 1,000,000 Hz with 50 mV of amplitude at constant potential of 0 V.

2.3. Methods

2.3.1. Preparation of s-SWCNTs/GCE

GCE was first polished with 1, 0.3 and 0.05 µm alumna slurry on a microcloth pad and then rinsed with double distilled water (ddH_2O). Subsequently, GCE was cleaned by bath sonication in sulphuric acid:water (1:1, v/v) and ethanol:water (1:1, v/v) for 1 min and then

ACCEPTED MANUSCRIPT

rinsed with ddH_2O and allowed to dry by N_2 gas. Finally, GCE was immersed in 10 mL of methanol solution containing 1% APTES for 30 min at room temperature. After that, APTES functionalized GCE was taken out and dried with nitrogen gas. Then, 10 µL of s-SWCNTs was drop casted on the APTES/GCE and dryied at room temperature (**Scheme 1A)** [52]. Hereafter, it is denoted as s-SWCNTs/GCE.

2.3.2. Biosensor fabrication

The s-SWCNTs/GCE was immersed in 2.5% glutaraldehyde (Glu) solution for 30 min. Followed by, 10 µL of AChE (0.01 mg/mL in 20 mM of PBS solution at pH 7.4) was coated on the Glu-s-SWCNTs/GCE surface and allowed to incubate for 30 min at 4° C. In addition, to block the nonspecific binding sites, 10 µL of BSA (0.01 mg/mL in 100 mM PBS solution at pH 7.4) was coated on AChE-Glu-s-SWCNTs/GCE surface and allowed to incubate for 30 min at 4° C. Finally, the BSA/AChE-Glu-s-SWCNTs/GCE was rinsed with 100 mM PBS (pH 7.4) and stored at 4° C (**Scheme 1A**). In addition, BSA/AChE-s-SWCNTs/GCE and s-SWCNTs/GCE were also prepared for comparison studies.

2.3.3. Biosensor assay procedure

The BSA/AChE-Glu-s-SWCNTs/GCE was used as a working electrode. 10 mL of 100 mM PBS electrolyte solution (pH 7.4) was utilized for all experiments. CV and SWV measurements were made after 15 min of incubation in PBS. The optimum concentration of ATCl (4 mM) was added into the PBS (100 mM, pH 7.4) solution. Thereafter, various concentrations of MP pesticide were added to the electrochemical cell containing 4 mM ATCl with PBS (pH 7.4) for the analysis. The SWV current responses were decreased against various concentrations of MP due to the inhibition of enzyme activity (**Scheme 1**). In this study, PBS (pH 7.4) was selected as an electrolyte, because it offers physiological condition for biosensor assay in neutral medium and AChE (acid labile) is also more reactive in this pH range [53–55].

ACCEPTED MANUSCRIPT

3. RESULTS AND DISCUSSION

3.1. UV-vis-NIR analysis

UV-vis-NIR spectroscopy has been broadly utilized to analyse the pristine SWCNTs and s-SWCNTs (**Fig. 1A, curves i and ii**) [52]. The first inter-band transition (M_{11}) (620 to 780 nm) peak represents metallic nanotubes, and the second and third inter-band transitions were due to S_{33} (420-580 nm) and S_{22} (820-1200 nm) semiconducting nanotubes [56]. For the obtained s-SWCNTs sample (**Fig. 1A, curve ii**), the peak corresponding to the first inter-band transition of metallic SWCNTs is completely disappeared (due to the removal of metallic nanotubes). It has been confirmed that the obtained solution was highly pure s-SWCNTs [52].

3.2. Raman spectroscopy and TEM analysis

The above UV-vis-NIR data is also supported by the Raman spectra presented in **Fig. 1B,** in which a clear radial breathing mode (RBM) peaks were observed between 130 – 240 cm^{-1} for the s-SWCNTs (**Fig. 1B, curve ii**) than pristine SWCNTs (**Fig. 1B, curve i**) (confirming that the enrichment of semiconducting nanotubes) [52,56,57]. The Raman signatures in the frequency range between 1450 – 1700 cm^{-1} (**Fig. 1B**) showed the nanotube tangential modes with the characteristic G^- and G^+ features [56]. For the s-SWCNTs (**Fig. 1B, curve ii**), G^- peak was observed at 1566.77 cm^{-1}, which was related to the decrease in the intensity of the Breit-Wigner-Fano peak from the pristine SWCNTs (**Fig. 1B, curve i**). It corroborated that metallic nanotube content is diminished in s-SWCNTs [56,58,59]. Furthermore, the short Raman D band indicated that the s-SWCNTs contain less structural defects [60].

For HR-TEM analysis, a carbon-coated copper grid was modified with 10 µL of s-SWCNTs solution and dried at room temperature. **Fig. 1C** shows the HR-TEM image of pure s-SWCNTs. Several individual nanotubes with average length of 1 µm were observed which indicated highly dispersed nanotubes present in the s-SWCNTs solution [61].

ACCEPTED MANUSCRIPT

3.3. FT-IR study of the s-SWCNTs and AChE-Glu-s-SWCNTs.

Fig. 2(**A and B**) shows FT-IR spectra of s-SWCNTs and AChE-Glu-s-SWCNTs films coated on silica substrates. The IR absorption bands were reported for amide I groups (1610-1690 cm^{-1}) corresponding to the C=O stretching vibration, amide II (1500-1600 cm^{-1}) and amide III (1310-1390 cm^{-1}) groups from a combination of N-H bending and C-N stretching vibration of peptide linkage of proteins [62–64]. The FT-IR spectrum of AChE-Glu-s-SWCNTs film showed three absorption peaks at 1675 cm^{-1}, 1592 cm^{-1} and 1370 cm^{-1}, which corresponded to the amide I, amide II and amide III groups of the proteins on enzyme membrane adsorbed on Glu-s-SWCNTs which proved that AChE retained its native structure (**Fig. 2A**). The FT-IR spectrum of AChE-Glu-s-SWCNTs is also showed a new peak at 1729 cm^{-1} and 1400 cm^{-1} confirmed the presence of C=N bond and hence immobilization of AChE via $–NH_2$ group, introduced by Glu on s-SWCNTs surface (**Fig. 2A**) [63,64]. In addition, a broad and weak band appeared at 3511 cm^{-1} and 3073 cm^{-1} which can be associated to N-H stretching modes [63,64] of the attached AChE protein (**Fig. 2B**). The attachments of aliphatic groups are highlighted by C–H asymmetric and symmetric stretching modes observed at 2865 cm^{-1} and 2940 cm^{-1} [63,64]. This proved that Glu molecules are well connected with AChE and s-SWCNTs film (**Fig. 2B**).

3.4. CV and EIS analysis

CV and EIS were carried out in 100 mM KCl containing 5 mM $K_3[Fe(CN)_6]$ and 5 mM $K_4[Fe(CN)_6]$ to characterize the interfacial electrochemical properties of different modified electrodes such as bare GCE, s-SWCNTs/GCE, BSA/AChE-s-SWCNTs/GCE and BSA/AChE-Glu-s-SWCNTs/GCE (**Fig. 3**). Cyclic voltammograms (CVs) of aforementioned electrodes showed a typical sigmoidal shape with narrow peak potential separations. Additionally, each fabricated electrode showed a different CV peak currents and potentials shift which indicated the stepwise assembly process of the biosensor. The peak potential separation (ΔEp) at bare GCE, s-SWCNTs/GCE, BSA/AChE-s-SWCNTs/GCE and

BSA/AChE-Glu-s-SWCNTs/GCE were obtained as 0.147 V, 0.134 V, 0.108 V and 0.116 V, respectively (**Fig. 3A**).

After modification with s-SWCNTs/GCE, ΔEp is decreased to 0.134 V with a noticeable increase in the redox peak currents compared to bare GCE (**Fig. 3A, curves a, b**). This was due to high carrier mobility, mechanical stability and scattering free ballistic transport properties of s-SWCNTs [34–36,65]. For BSA/AChE-s-SWCNTs/GCE, the reversible redox peak currents obviously increased and the ΔEp separation decreased to 0.108 V (**Fig. 3A, curve c**) compared with other modified electrodes (**Fig. 3A**). Hence, the improved reversibility of redox system was attributed due to higher charge transfer property and reduction of mass transfer resistivity on GCE. However, after incorporating BSA/AChE-Glu-s-SWCNTs onto GCE, the reversible redox peak currents significantly decreased and the ΔEp increased to 0.116 V (**Fig. 3A, curve d**) compared with BSA/AChE-s-SWCNTs/GCE. This may be due to less interaction between BSA/AChE-Glu-s-SWCNTs/GCE and $K_3[Fe(CN)_6]$ and $K_4[Fe(CN)_6]$ [66].

The observed changes in the interfacial impedance of different modified electrodes was probed at each step of electrode fabrication using EIS (**Fig. 3B**). A typical Nyquist plot is composed of a semicircle and linear part observed at higher and lower frequencies, corresponds to the electron transfer limited process and diffusion limited process [67]. **Fig. 3B** illustrates typical Nyquist plots of bare GCE, s-SWCNTs/GCE, BSA/AChE-s-SWCNTs/GCE and BSA/AChE-Glu-s-SWCNTs/GCE using $[Fe(CN)_6]^{3-/4-}$ as a redox probe. The charge transfer resistance (R_{CT}) can be obtained by calculating the diameter of the semicircle [67]. According to the calculation, the R_{CT} of different modified electrodes such as bare GCE, s-SWCNTs/GCE, BSA/AChE-s-SWCNTs/GCE and BSA/AChE-Glu-s-SWCNTs/GCE were obtained as 110.81 Ω (**curve a**), 104.52 Ω (**curve b**), 85.91 Ω (**curve c**) and 96.62 Ω (**curve d**), respectively. [66]. It was evident that s-SWCNTs based electrode

ACCEPTED MANUSCRIPT

[35] improved charge transfer property and reduction of mass transfer resistivity (**curves c & d**) [68,69].

3.5. Electrochemical oxidation of ATCl

The SWV of BSA/AChE-Glu-s-SWCNTs/GCE was recorded in the 100 mM PBS (pH 7.4) containing ATCl under nitrogen atmosphere. **Fig. 4** shows a strong oxidation peak at + 0.62 V for 4 mM ATCl. At the same time, there was no notable current response in the absence of ATCl. Next, the anodic peak current changes were plotted against different concentrations of ATCl from 1 mM to 8 mM (**Fig. S1 of the supporting information**). The oxidation peak currents were increased up to 4 mM of ATCl. There was no notable changes in anodic peak current after 4 mM of ATCl. It indicated that the proposed biosensor had reached its saturation level. Based on the above results, 4 mM ATCl was selected as an optimum concentration for biosensor measurements. Furthermore, suitable incubation period for ATCl oxidation was analysed between 0 to 30 min and 15 min was selected as a suitable incubation time period.

Fig. 5 shows the CVs of various modified electrodes in 100 mM PBS (pH 7.4) with an optimum concentration of ATCl. As anticipated, no anodic current response (oxidation peak) was observed at BSA/AChE-Glu-s-SWCNTs/GCE in the absence of ATCl in PBS solution (**Fig. 4**). However, after addition of ATCl into PBS, BSA/AChE-Glu-s-SWCNTs/GCE exhibited an irreversible oxidation peak due to the oxidation of Thiocholine (TCh) which yields a hydrolysis compound of ATCl, catalysed by the presence of AChE enzyme. The electrochemical response observed at the proposed biosensor surface was based on the following reactions (**Scheme 1**B) [46].

For comparison, BSA/AChE-s-SWCNTs/GCE is also showed a significant oxidation peak current (**Fig. 5, curve c**). However, this oxidation peak current was lower than proposed BSA/AChE-Glu-s-SWCNTs/GCE (**Fig. 5, curve d**). The enhanced oxidation peak current of

TCh recorded at BSA/AChE-Glu-s-SWCNTs/GCE could be credited to the presence of Glu on s-SWCNTs. Because, it could easily attract the amide group-containing organic compounds which could help to immobilize AChE enzyme on the s-SWCNTs and improved the electrochemical reactions [48,50]. In addition, GCE surface has been functionalized with APTES which is known to enhance the binding of nanotube and improve the performance of biosensor [70]. Meanwhile, TCh oxidation peak did not appear on s-SWCNTs/GCE (**Fig. 5, curve b**) and bare GCE (**Fig. 5, curve a**) because of the absence of AChE enzyme. The above results confirmed that Glu cross-linked between s-SWCNTs and AChE have improved the electrocatalytic performance of the biosensor.

The effect of scan rates on BSA/AChE-Glu-s-SWCNTs/GCE in 100 mM PBS solution containing 4 mM ATCl was studied (**Fig. 6**). Based on CV results, with the scan rate from 10 mV s^{-1} to 100 mV s^{-1}, oxidation peak currents of TCh were increased and oxidation potentials gradually shifted to positive direction (**Fig. 6)**. This indicated that the oxidation of ATCl on BSA/AChE-Glu-s-SWCNTs/GCE is a diffusion-controlled process [71]. From this study, 100 mVs^{-1} was selected as an optimum scan rate for further analysis due to distinct oxidation peak of TCh. The plot obtained between TCh oxidation peak current (I_{pa}) *vs.* square roots of scan rate ($v^{1/2}$) demonstrated a good linearity which confirmed the diffusion controlled oxidation process (R^2=0.9951, n=3) (**Fig. 6).**

3.6. Pesticide detection

MP pesticide was naturally inhibiting the AChE enzyme reaction [72]. The enzymatic inhibition measurements were performed under the optimum condition of 4 mM ATCl with PBS using the proposed BSA/AChE-Glu-s-SWCNTs/GCE biosensor. The oxidation peak current of ATCl was decreased after the interaction with pesticide in electrochemical cell which clearly indicated enzyme–pesticide binding at BSA/AChE-Glu-s-SWCNTs/GCE biosensor. In SWV, oxidation peak was decreased with inhibition of the AChE enzyme activity by the different concentrations of MP (**Fig. 7**). The decrease in the oxidation peak

ACCEPTED MANUSCRIPT

current can be attributed to the presence of covalently bound phosphate group-containing MP is effectively blocking the serine hydroxyl group of AChE enzyme, which invariably reduces the ATCl oxidation (decrease of TCh product) [48]. To estimate the performance of the proposed biosensor (BSA/AChE-Glu-s-SWCNTs/GCE) for MP detection, the SWV anodic net current responses were noted with different concentrations of MP (**Fig. 7**). As shown in inset of Fig. 7, the net current response was decreased linearly with the increasing of MP concentrations from 1×10^{-10} M to 5×10^{-6} M (correlation coefficient, R^2 was 0.9825; n=3). Furthermore, the limit of detection (LOD) of MP was calculated to be 3.75×10^{-11} M using the following equation 1 [73].

$$LOD = 3SD/S \quad (1)$$

Where, SD is the standard deviation of blank (2.25×10^{-7} A) and S is the slope of the calibration curve (1.8×10^{-8} A pM^{-1}). The calculated LOD (3.75×10^{-11} M) is comparable with the other reported methods for MP by enzymatic/non-enzymatic sensors as given in **Table 1**. It is clear that, the proposed biosensor was doable with the lowest MP detection, and this detection level is less than the allowable pesticide limits as set by environmental protection agency's [9]. In addition, non-enzymatic MP sensors can detect MP up to up to 0.5×10^{-9} M concentration. But, enzymatic MP sensors were better than non-enzymatic sensors which is due to high sensitivity and selectivity of compounds or preferentially binding the target [18,45–47,74–77]. Our fabricated s-SWCNT based biosensor showed enhanced electrochemical reaction with MP via simple enzyme immobilization which retained the enzyme activity as a potential biosensor. It is possible to extend the same procedure to detect other organophosphorus pesticides using this approach. Other semiconducting materials can also be used for biosensor fabrication. This new method opens up new possibilities for the designing of s-SWCNTs-FET based electrochemical biosensor for detection of pesticides.

3.7. Selectivity, stability, reproducibility and repeatability

ACCEPTED MANUSCRIPT

The selectivity of BSA/AChE-Glu-s-SWCNTs/GCE biosensor was evaluated by SWV measurements. As displayed in the **Fig. 8**, the proposed biosensor was exposed to the optimum concentration of ATCl with PBS as a blank. The blank measurements showed predominant oxidation peak at + 0.62 V. After that, proposed biosensors oxidation peak current did not significantly affected by the addition of other organic compounds such as glucose (GU), uric acid (UA) and oxalic acid (OA) (**Fig. 8A**), which indicated that proposed biosensor effectively eliminated the interferent and did not allow the electron transfer process from electrolyte to electrode interface. However, SWV anodic current response (relative signal intensity) was decreased about 4.8% in the presence of ascorbic acid (AA). It might be attributed to the biochemical reaction of AA (reducing agent) by donating electrons to the AChE enzymatic reactions which invariably convert ascorbic acid to dehydroascorbic acid or semi dehydroascorbic acid. Because of this side reaction, it slightly reduced the AChE enzyme activity (**Fig. 8B**) [78]. Moreover, in presence of orthophosphoric acid (OPA), the relative signal intensity was decreased about only 1.7%. It was due to the presence of conjugated base hydrogen phosphate group which slightly reduced the AChE enzyme activity (**Fig. 8B**) [79].

Furthermore, the storage stability of the fabricated biosensor was studied by SWV (**Fig. 9A**). The proposed biosensor was stored in 100 mM PBS (pH 7.4) at 4°C in the refrigerator. The oxidation current intensity changes were recorded before and after storage for certain periods in the refrigerator. The fabricated biosensor showed about 6.86% decrease in response after storage of 33 days (**Fig. 9B**). This study suggested that fabricated biosensor is relatively stable and maybe be suitable for long time usage. Moreover, the reproducibility and repeatability of the biosensor were also investigated. Three different biosensors were prepared independently and used for the detection of 5×10^{-10} M MP in 100 mM PBS (pH 7.4). The relative standard deviation (RSD) was 4.68%. Next, the same biosensor was used for repetitive determination of MP for three consecutive measurements. The observed data

resulted an RSD of 0.89% for n=3. This study proved that the proposed biosensor is suitable for MP detection (**Table S1 of the supporting information**).

3.8. Real sample analysis

Figs. S2 & S3 (Supporting information) displays the SWV responses obtained for the MP detection in strawberry and apple fruit samples using BSA/AChE-Glu-s-SWCNTs/GCE biosensor. As shown, the anodic current responses were decreased with increasing MP concentration from 1×10^{-10} M to 5×10^{-6} M (**Fig. S2**) and 5×10^{-10} M to 5×10^{-6} M (**Fig. S3**). The linear current responses were attained with a correlation coefficient (R^2) of 0.989 and 0.933. The recovery of MP was between 98.31% and 102.22% with the RSD of 1.72% and 4.53%, respectively (**Table S1**). In some measurements, the spiked MP concentration was found lesser than expected which was due to the presence of common interferent and some impurities. However, recovery results for MP were acceptable in strawberry and apple fruit samples. These results confirmed that the proposed biosensor is suitable for real sample analysis. In addition, proposed biosensor (BSA/AChE-Glu-s-SWCNTs/GCE) fabrication and detection procedures are simple and effective compared to other methods, i.e. liquid/gas chromatography [12], mass spectrometry [11], colorimetry [10], Raman [13], photoluminescence and fluorescence spectroscopies [14,15].

4. CONCLUSIONS

The proposed BSA/AChE-Glu-s-SWCNTs/GCE biosensor is demonstrated with superior selectivity and sensitivity for MP detection than BSA/AChE-s-SWCNTs/GCE, s-SWCNTs/GCE and bare GCE. In addition, s-SWCNTs are not only offered the effective electron transfer process but also increased surface area for successful assembling of Glu/AChE/BSA. The BSA film on AChE-Glu-s-SWCNTs acted as a good protective layer to AChE enzyme from by-product of acetic acid. The proposed biosensor exhibited excellent sensing performance toward MP with a wide linear range of detection (1×10^{-10} M to 5×10^{-6} M) and lower LOD (3.75×10^{-11} M). Moreover, the proposed biosensor was applied for MP

ACCEPTED MANUSCRIPT

detection in strawberry and apple fruit samples which demonstrated that this method can be applied for real-world samples. We envisage that the proposed MP biosensor (BSA/AChE-Glu-s-SWCNTs/GCE) could be effectively utilized for food quality monitoring. In addition, for the first time, we have successfully demonstrated that pure s-SWCNT based biosensor can be used for detection of MP pesticide. However, further studies are required to make a switchable s-SWCNTs-FET with similar modification (BSA/AChE-Glu-s-SWCNTs) to fabricate prototype pesticide sensor for food and environmental safety/quality monitoring applications.

5. ASSOCIATED CONTENT

5.1 Supporting information

Preparation of MP pesticide stock solution and real sample assay preparation procedure, MP pesticide detection in apple and strawberry fruit samples were provided. Table of calculated RSD and recovery analysis for MP in apple and strawberry fruit samples is provided.

6. AUTHOR INFORMATION

Corresponding Author

*E-mail: ashokkumar.sun@ktr.srmuniv.ac.in.

ORCID

Ashok K. Sundramoorthy: 0000-0002-8512-9393

Notes

The authors declare no competing financial interest.

7. ACKNOWLEDGEMENTS

We acknowledge the Science and Engineering Research Board (SERB), Government of India for the funding through Early Career Research Award (Ref. No.: ECR/2016/001446). We also thank SRM Institute of Science and Technology for providing laboratory facilities to carry out this research project. T.H.V appreciates SERB for supporting project assistant fellowship through the ECRA grant.

8. REFERENCES

[1] L. Horrigan, R.S. Lawrence, P. Walker, How sustainable agriculture can address the environmental and human health harms of industrial agriculture., Environ. Health Perspect. 110 (2002) 445.

[2] P. Howard, Handbook of environmental fate and exposure data: for organic chemicals, volume III pesticides, Routledge, 2017.

[3] T.H.V. Kumar, S.K. Yadav, A.K. Sundramoorthy, Electrochemical Synthesis of 2D Layered Materials and Their Potential Application in Pesticide Detection, J. Electrochem. Soc. 165 (2018) B848–B861.

[4] A.K. Sundramoorthy, T.H.V. Kumar, S. Gunasekaran, Graphene-Based Nanosensors and Smart Food Packaging Systems for Food Safety and Quality Monitoring, in: Graphene Bioelectron., Elsevier, 2018: pp. 267–306.

[5] M. Eddleston, N.A. Buckley, P. Eyer, A.H. Dawson, Management of acute organophosphorus pesticide poisoning, Lancet. 371 (2008) 597–607.

[6] M. Kah, R.S. Kookana, A. Gogos, T.D. Bucheli, A critical evaluation of nanopesticides and nanofertilizers against their conventional analogues, Nat. Nanotechnol. (2018) 1.

[7] E. Forum, Killer environment, Env. Heal. Perspect. 107 (1999) A62.

[8] EPA, EPA United States Environmental Protection Agency (https://www.epa.gov/safepestcontrol/food-and-pesticides) (2017).

[9] D. Barceló, Environmental Protection Agency and other methods for the determination of priority pesticides and their transformation products in water, J. Chromatogr. A. 643 (1993) 117–143.

[10] X. Wang, Y. Yang, J. Dong, F. Bei, S. Ai, Lanthanum-functionalized gold nanoparticles for coordination–bonding recognition and colorimetric detection of

ACCEPTED MANUSCRIPT

methyl parathion with high sensitivity, Sensors Actuators B Chem. 204 (2014) 119–124.

[11] C. Ferrer, M.J. Gómez, J.F. García-Reyes, I. Ferrer, E.M. Thurman, A.R. Fernández-Alba, Determination of pesticide residues in olives and olive oil by matrix solid-phase dispersion followed by gas chromatography/mass spectrometry and liquid chromatography/tandem mass spectrometry, J. Chromatogr. A. 1069 (2005) 183–194.

[12] M.R. Khalili-Zanjani, Y. Yamini, N. Yazdanfar, S. Shariati, Extraction and determination of organophosphorus pesticides in water samples by a new liquid phase microextraction–gas chromatography–flame photometric detection, Anal. Chim. Acta. 606 (2008) 202–208.

[13] D. Lee, S. Lee, G.H. Seong, J. Choo, E.K. Lee, D.-G. Gweon, S. Lee, Quantitative analysis of methyl parathion pesticides in a polydimethylsiloxane microfluidic channel using confocal surface-enhanced Raman spectroscopy, Appl. Spectrosc. 60 (2006) 373–377.

[14] J. Hou, J. Dong, H. Zhu, X. Teng, S. Ai, M. Mang, A simple and sensitive fluorescent sensor for methyl parathion based on l-tyrosine methyl ester functionalized carbon dots, Biosens. Bioelectron. 68 (2015) 20–26.

[15] C.I.L. Justino, A.C. Duarte, T.A.P. Rocha-Santos, Recent progress in biosensors for environmental monitoring: A review, Sensors. 17 (2017) 2918.

[16] J. Wang, Carbon□nanotube based electrochemical biosensors: A review, Electroanal. 17 (2005) 7–14.

[17] M. Pumera, S. Sánchez, I. Ichinose, J. Tang, Electrochemical nanobiosensors, Sensors Actuators, B Chem. 123 (2007) 1195–1205.

[18] M. Govindasamy, V. Mani, S.-M. Chen, T.-W. Chen, A.K. Sundramoorthy, Methyl parathion detection in vegetables and fruits using silver@ graphene nanoribbons nanocomposite modified screen printed electrode, Sci. Rep. 7 (2017) 46471.

ACCEPTED MANUSCRIPT

[19] Y. Shao, J. Wang, H. Wu, J. Liu, I.A. Aksay, Y. Lin, Graphene Based Electrochemical Sensors and Biosensors : A Review, (2010) 1027–1036.

[20] S. Dong, L. Peng, W. Wei, T. Huang, Three MOF-Templated Carbon Nanocomposites for Potential Platforms of Enzyme Immobilization with Improved Electrochemical Performance, ACS Appl. Mater. Interfaces. 10 (2018) 14665–14672.

[21] L. Li, L. Wang, Q. Xu, L. Xu, W. Liang, Y. Li, M. Ding, A. Aldalbahi, Z. Ge, L. Wang, Bacterial analysis using an electrochemical DNA biosensor with Poly-adenine-mediated DNA self-assembly, ACS Appl. Mater. Interfaces. 10 (2018) 6895–6903.

[22] J.A. Hondred, J.C. Breger, N.J. Alves, S.A. Trammell, S.A. Walper, I.L. Medintz, J.C. Claussen, Printed graphene electrochemical biosensors fabricated by inkjet maskless lithography for rapid and sensitive detection of organophosphates, ACS Appl. Mater. Interfaces. 10 (2018) 11125–11134.

[23] A.K. Sundramoorthy, S. Gunasekaran, Partially Oxidized Graphene/Metallic Single□ Walled Carbon Nanotubes Film□Coated Electrode for Nanomolar Detection of Dopamine, Electroanalysis. 27 (2015) 1811–1816.

[24] S.A. Kumar, S.-L. Chen, S.-M. Chen, Electrochemical Sensing of H_2O_2 at flavin adenine dinucleotide/chitosan/CNT nanocomposite modified electrode, Electrochem. Solid-State Lett. 13 (2010) K83–K86.

[25] A.K. Sundramoorthy, O. Sadak, S. Anandhakumar, S. Gunasekaran, Synthesis of poly (8-aminopyrene-1, 3, 6-trisulfonic acid)/CNT Nanocomposite for Electrochemical Detection of Caffeine, J. Electrochem. Soc. 163 (2016) B638–B643.

[26] S.A. Kumar, S.L. Chen, S.M. Chen, Nanostructured Materials, Carbon Nanotubes, and Fullerenes Electrochemical Sensing of H2O2 at Flavin Adenine Dinucleotide/Chitosan/CNT Nanocomposite Modified Electrode, IEEE-ECS Electrochem. Solid State Lett. 13 (2010) K83.

[27] T.H.V. Kumar, A.K. Sundramoorthy, Non-Enzymatic Electrochemical Detection of

Urea on Silver Nanoparticles Anchored Nitrogen-Doped Single-Walled Carbon Nanotube Modified Electrode, J. Electrochem. Soc. 165 (2018) B3006–B3016.

[28] P. Prakash, K.M. Sundaram, M.A. Bennet, A review on carbon nanotube field effect transistors (CNTFETs) for ultra-low power applications, Renew. Sustain. Energy Rev. 89 (2018) 194–203.

[29] J. Si, D. Zhong, H. Xu, M. Xiao, C. Yu, Z. Zhang, L.-M. Peng, Scalable Preparation of High-Density Semiconducting Carbon Nanotube Arrays for High-Performance Field-Effect Transistors, ACS Nano. 12 (2018) 627–634.

[30] S. Farhana, Novel carbon nanotube model for low energy loss field-effect transistor, Cogent Eng. 4 (2017) 1300082.

[31] C. Wang, K. Takei, T. Takahashi, A. Javey, Carbon nanotube electronics–moving forward, Chem. Soc. Rev. 42 (2013) 2592–2609.

[32] M.F.L. De Volder, S.H. Tawfick, R.H. Baughman, A.J. Hart, Carbon nanotubes: present and future commercial applications, Science 339 (2013) 535–539.

[33] J.-W. Oh, J. Heo, T.H. Kim, An electrochemically modulated single-walled carbon nanotube network for the development of a transparent flexible sensor for dopamine, Sensors Actuators B Chem. 267 (2018) 438–447.

[34] V. Perebeinos, J. Tersoff, P. Avouris, Electron-phonon interaction and transport in semiconducting carbon nanotubes, Phys. Rev. Lett. 94 (2005) 86802.

[35] J. Cao, Q. Wang, H. Dai, Electromechanical properties of metallic, quasimetallic, and semiconducting carbon nanotubes under stretching, Phys. Rev. Lett. 90 (2003) 157601.

[36] T. Dürkop, S.A. Getty, E. Cobas, M.S. Fuhrer, Extraordinary mobility in semiconducting carbon nanotubes, Nano Lett. 4 (2004) 35–39.

[37] H.R. Byon, H.C. Choi, Network single-walled carbon nanotube-field effect transistors (SWNT-FETs) with increased Schottky contact area for highly sensitive biosensor applications, J. Am. Chem. Soc. 128 (2006) 2188–2189.

ACCEPTED MANUSCRIPT

[38] M.J. Kiani, M.A.A. Razak, F.K. Harun, M.T. Ahmadi, M. Rahmani, SWCNT-based biosensor modelling for pH detection, J. Nanomater. 16 (2015) 102.

[39] D. Son, J.H. Koo, J.-K. Song, J. Kim, M. Lee, H.J. Shim, M. Park, M. Lee, J.H. Kim, D.-H. Kim, Stretchable carbon nanotube charge-trap floating-gate memory and logic devices for wearable electronics, ACS Nano. 9 (2015) 5585–5593.

[40] C. Biswas, Y.H. Lee, Graphene versus carbon nanotubes in electronic devices, Adv. Funct. Mater. 21 (2011) 3806–3826.

[41] M. Sireesha, V. Jagadeesh Babu, A.S. Kranthi Kiran, S. Ramakrishna, A review on carbon nanotubes in biosensor devices and their applications in medicine, Nanocomposites. 4 (2018) 36–57.

[42] W.-S. Li, P.-X. Hou, C. Liu, D.-M. Sun, J. Yuan, S.-Y. Zhao, L.-C. Yin, H. Cong, H.-M. Cheng, High-quality, highly concentrated semiconducting single-wall carbon nanotubes for use in field effect transistors and biosensors, ACS Nano. 7 (2013) 6831–6839.

[43] W. Aktar, D. Sengupta, A. Chowdhury, Impact of pesticides use in agriculture: their benefits and hazards, Interdiscip. Toxicol. 2 (2009) 1–12.

[44] S. Song, L. Wang, J. Li, C. Fan, J. Zhao, Aptamer-based biosensors, TrAC Trends Anal. Chem. 27 (2008) 108–117.

[45] J. Gong, Z. Guan, D. Song, Biosensor based on acetylcholinesterase immobilized onto layered double hydroxides for flow injection/amperometric detection of organophosphate pesticides, Biosens. Bioelectron. 39 (2013) 320–323.

[46] R. Xue, T.-F. Kang, L.-P. Lu, S.-Y. Cheng, Immobilization of acetylcholinesterase via biocompatible interface of silk fibroin for detection of organophosphate and carbamate pesticides, Appl. Surf. Sci. 258 (2012) 6040–6045.

[47] L. Yang, G. Wang, Y. Liu, M. Wang, Development of a biosensor based on immobilization of acetylcholinesterase on NiO nanoparticles–carboxylic graphene–

ACCEPTED MANUSCRIPT

nafion modified electrode for detection of pesticides, Talanta. 113 (2013) 135–141.

[48] S. Viswanathan, H. Radecka, J. Radecki, Electrochemical biosensor for pesticides based on acetylcholinesterase immobilized on polyaniline deposited on vertically assembled carbon nanotubes wrapped with ssDNA, Biosens. Bioelectron. 24 (2009) 2772–2777.

[49] G. Liu, Y. Lin, Biosensor Based on Self-Assembling Acetylcholinesterase on Carbon Nanotubes for Flow Injection/Amperometric Detection of Organophosphate Pesticides and Nerve Agents, Anal. Chem. 78 (2006) 835–843.

[50] R. Pauliukaite, M.E. Ghica, O. Fatibello-Filho, C.M.A. Brett, Comparative study of different cross-linking agents for the immobilization of functionalized carbon nanotubes within a chitosan film supported on a graphite− epoxy composite electrode, Anal. Chem. 81 (2009) 5364–5372.

[51] I. Migneault, C. Dartiguenave, M.J. Bertrand, K.C. Waldron, Glutaraldehyde: behavior in aqueous solution, reaction with proteins, and application to enzyme crosslinking, Biotechniques. 37 (2004) 790–802.

[52] J. Wang, T.D. Nguyen, Q. Cao, Y. Wang, M.Y.C. Tan, M.B. Chan-Park, Selective surface charge sign reversal on metallic carbon nanotubes for facile ultrahigh purity nanotube sorting, ACS Nano. 10 (2016) 3222–3232.

[53] S.M. Sultan, M.R.R. de Planque, P. Ashburn, H.M.H. Chong, Effect of Phosphate Buffered Saline Solutions on Top-Down Fabricated ZnO Nanowire Field Effect Transistor, J. Nanomater. 2017 (2017).

[54] A. Bhide, S. Cheeran, S. Muthukumar, S. Prasad, Enzymatic Low Volume Passive Sweat Based Assays for Multi-Biomarker Detection, Biosensors. 9 (2019) 13.

[55] A. Alvarez, R. Alarcón, C. Opazo, E.O. Campos, F.J. Muñoz, F.H. Calderón, F. Dajas, M.K. Gentry, B.P. Doctor, F.G. De Mello, Stable complexes involving acetylcholinesterase and amyloid-β peptide change the biochemical properties of the

ACCEPTED MANUSCRIPT

enzyme and increase the neurotoxicity of Alzheimer's fibrils, J. Neurosci. 18 (1998) 3213–3223.

[56] A.K. Sundramoorthy, S. Mesgari, J. Wang, R. Kumar, M.A. Sk, S.H. Yeap, Q. Zhang, S.K. Sze, K.H. Lim, M.B. Chan-Park, Scalable and effective enrichment of semiconducting single-walled carbon nanotubes by a dual selective naphthalene-based azo dispersant, J. Am. Chem. Soc. 135 (2013) 5569–5581.

[57] M. V Kharlamova, Comparative analysis of electronic properties of tin, gallium, and bismuth chalcogenide-filled single-walled carbon nanotubes, J. Mater. Sci. 49 (2014) 8402–8411.

[58] W. Huang, F. Toshimitsu, K. Ozono, M. Matsumoto, A. Borah, Y. Motoishi, K.-H. Park, J.-W. Jang, T. Fujigaya, Thermoelectric properties of dispersant-free semiconducting single-walled carbon nanotubes sorted by a flavin extraction method, Chem. Commun. 55 (2019) 2636–2639.

[59] Y. Tian, H. Jiang, P. Laiho, E.I. Kauppinen, Validity of Measuring Metallic and Semiconducting Single-Walled Carbon Nanotube Fractions by Quantitative Raman Spectroscopy, Anal. Chem. 90 (2018) 2517–2525.

[60] M. Monthioux, Carbon meta-nanotubes: Synthesis, properties and applications, John Wiley & Sons, 2011.

[61] Y. Li, D. Mann, M. Rolandi, W. Kim, A. Ural, S. Hung, A. Javey, J. Cao, D. Wang, E. Yenilmez, Preferential growth of semiconducting single-walled carbon nanotubes by a plasma enhanced CVD method, Nano Lett. 4 (2004) 317–321.

[62] D. Du, J. Ding, J. Cai, A. Zhang, One-step electrochemically deposited interface of chitosan–gold nanoparticles for acetylcholinesterase biosensor design, J. Electroanal. Chem. 605 (2007) 53–60.

[63] M. Hiraoui, M. Guendouz, N. Lorrain, A. Moadhen, L. Haji, M. Oueslati, Spectroscopy studies of functionalized oxidized porous silicon surface for biosensing

applications, Mater. Chem. Phys. 128 (2011) 151–156.

[64] N. Chauhan, C.S. Pundir, Amperometric determination of acetylcholine—A neurotransmitter, by chitosan/gold-coated ferric oxide nanoparticles modified gold electrode, Biosens. Bioelectron. 61 (2014) 1–8.

[65] L. Ding, A. Tselev, J. Wang, D. Yuan, H. Chu, T.P. McNicholas, Y. Li, J. Liu, Selective growth of well-aligned semiconducting single-walled carbon nanotubes, Nano Lett. 9 (2009) 800–805.

[66] D. Du, X. Ye, J. Cai, J. Liu, A. Zhang, Acetylcholinesterase biosensor design based on carbon nanotube-encapsulated polypyrrole and polyaniline copolymer for amperometric detection of organophosphates, Biosens. Bioelectron. 25 (2010) 2503–2508.

[67] D. Song, Y. Wang, X. Lu, Y. Gao, Y. Li, F. Gao, Ag nanoparticles-decorated nitrogen-fluorine co-doped monolayer MoS_2 nanosheet for highly sensitive electrochemical sensing of organophosphorus pesticides, Sensors Actuators B Chem. 267 (2018) 5–13.

[68] R. Montes, F. Céspedes, D. Gabriel, M. Baeza, Electrochemical Biosensor Based on Optimized Biocomposite for Organophosphorus and Carbamates Pesticides Detection, J. Nanomater. 2018 (2018).

[69] P. Norouzi, M. Pirali-Hamedani, M.R. Ganjali, F. Faridbod, A novel acetylcholinesterase biosensor based on chitosan-gold nanoparticles film for determination of monocrotophos using FFT continuous cyclic voltammetry, Int. J. Electrochem. Sci. 5 (2010) 1434–1446.

[70] S.K. Raman Pillai, M.B. Chan-Park, High-performance printed carbon nanotube thin-film transistors array fabricated by a nonlithography technique using hafnium oxide passivation layer and mask, ACS Appl. Mater. Interfaces. 4 (2012) 7047–7054.

[71] H. Mehrer, Diffusion in solids: fundamentals, methods, materials, diffusion-controlled processes, Springer, Berlin heidelberg, 2007.

ACCEPTED MANUSCRIPT

[72] M.B. Colovic, D.Z. Krstic, T.D. Lazarevic-Pasti, A.M. Bondzic, V.M. Vasic, Acetylcholinesterase inhibitors: pharmacology and toxicology, Curr. Neuropharmacol. 11 (2013) 315–335.

[73] J. Yoon, E. Lee, D. Lee, T.-S. Oh, Y.S. Yoon, D.-J. Kim, Communication—Highly Sensitive Ag/ZnO Nanorods Composite Electrode for Non-Enzymatic Urea Detection, J. Electrochem. Soc. 164 (2017) B558–B560.

[74] B. Song, W. Cao, Y. Wang, A methyl parathion electrochemical sensor based on Nano-TiO2, graphene composite film modified electrode, Fullerenes Nanotub. Carbon Nanostructures. 24 (2016) 435–440.

[75] Y. Li, M. Xu, P. Li, J. Dong, S. Ai, Nonenzymatic sensing of methyl parathion based on graphene/gadolinium Prussian Blue analogue nanocomposite modified glassy carbon electrode, Anal. Methods. 6 (2014) 2157.

[76] A. Kumaravel, M. Chandrasekaran, A novel nanosilver/nafion composite electrode for electrochemical sensing of methyl parathion and parathion, J. Electroanal. Chem. 638 (2010) 231–235.

[77] L. Yang, G. Wang, Y. Liu, An acetylcholinesterase biosensor based on platinum nanoparticles–carboxylic graphene–nafion-modified electrode for detection of pesticides, Anal. Biochem. 437 (2013) 144–149.

[78] H. Tsukaguchi, T. Tokui, B. Mackenzie, U. V Berger, X.-Z. Chen, Y. Wang, R.F. Brubaker, M.A. Hediger, A family of mammalian Na+-dependent L-ascorbic acid transporters, Nature. 399 (1999) 70.

[79] Y.-H.P. Zhang, J. Cui, L.R. Lynd, L.R. Kuang, A transition from cellulose swelling to cellulose dissolution by o-phosphoric acid: evidence from enzymatic hydrolysis and supramolecular structure, Biomacromolecules. 7 (2006) 644–648.

Figure and captions

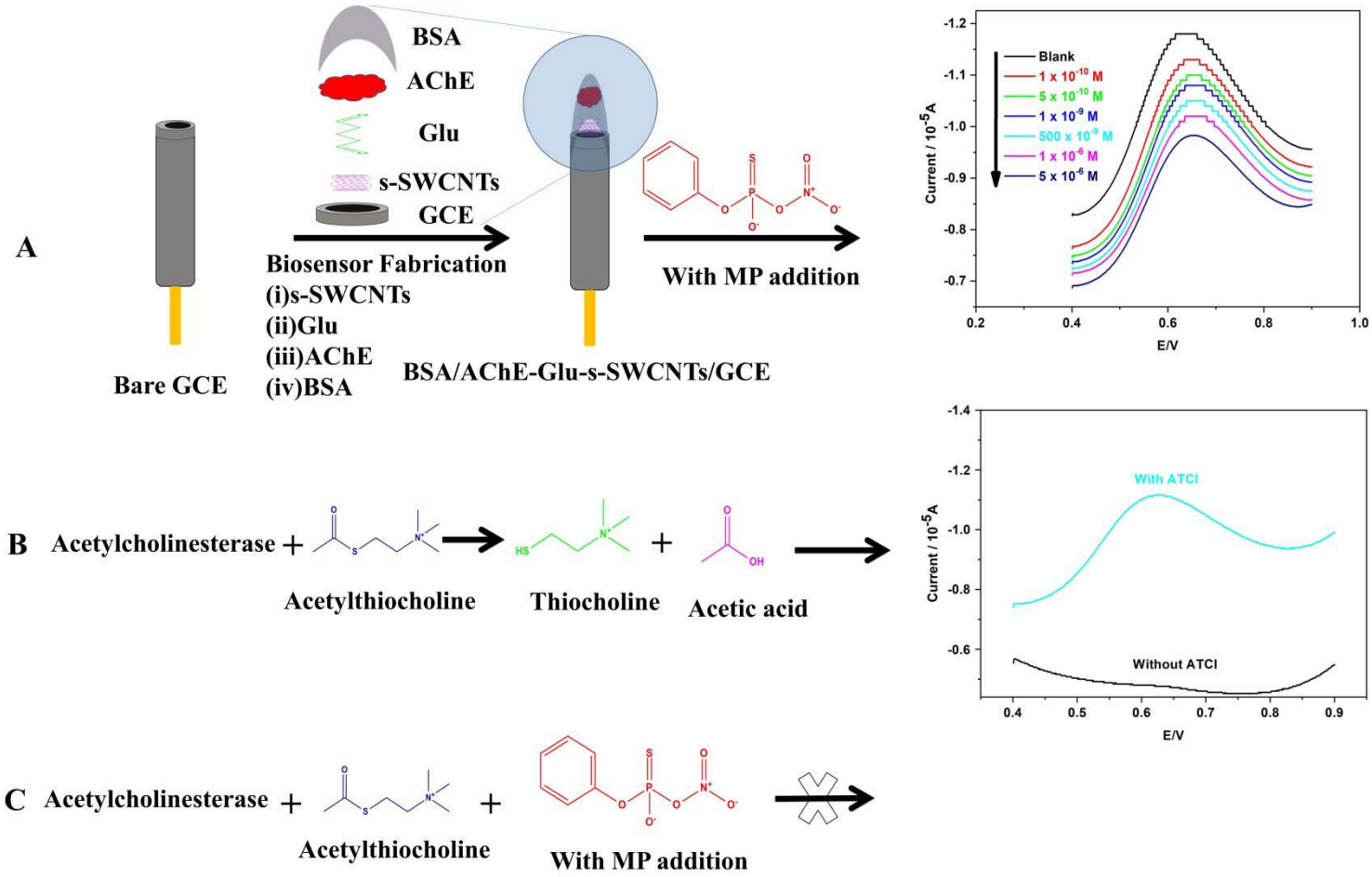

Scheme 1. Schematic illustration of BSA/AChE-Glu-s-SWCNTs/GCE biosensor fabrication and MP detection. **(A)** Preparation of BSA/AChE-Glu-s-SWCNTs/GCE for MP detection by SWV. **(B)** Electrochemical oxidation of ATCl on BSA/AChE-Glu-s-SWCNTs/GCE. **(C)** MP sensing mechanism at BSA/AChE-Glu-s-SWCNTs/GCE.

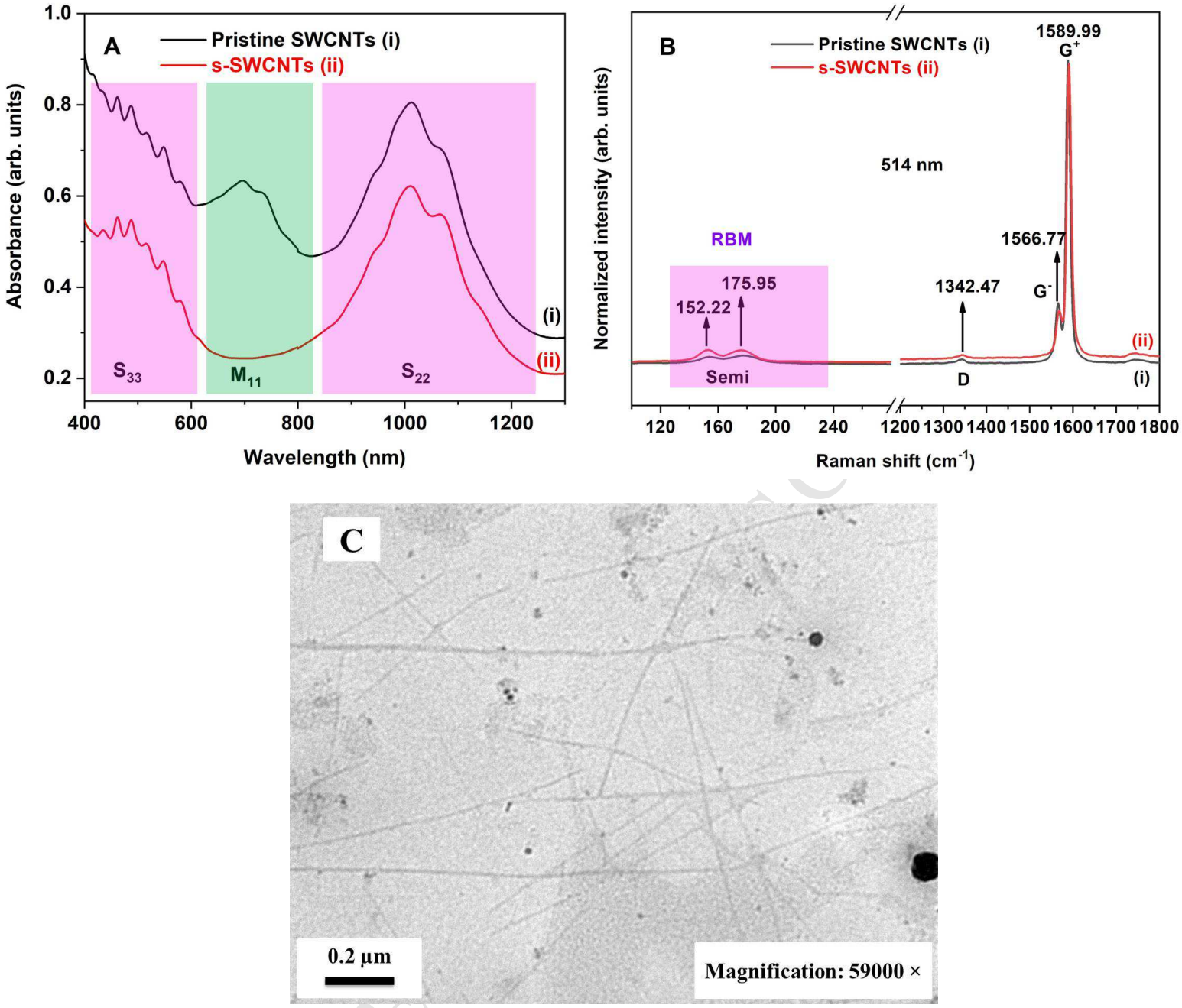

Fig. 1 (A) UV-vis-NIR spectra of pristine SWCNTs (i) and pure s-SWCNTs (ii). (**B**) Raman spectra of pristine SWCNTs (i) and pure s-SWCNTs (ii). (**C**) HR-TEM images of pure s-SWCNTs.

ACCEPTED MANUSCRIPT

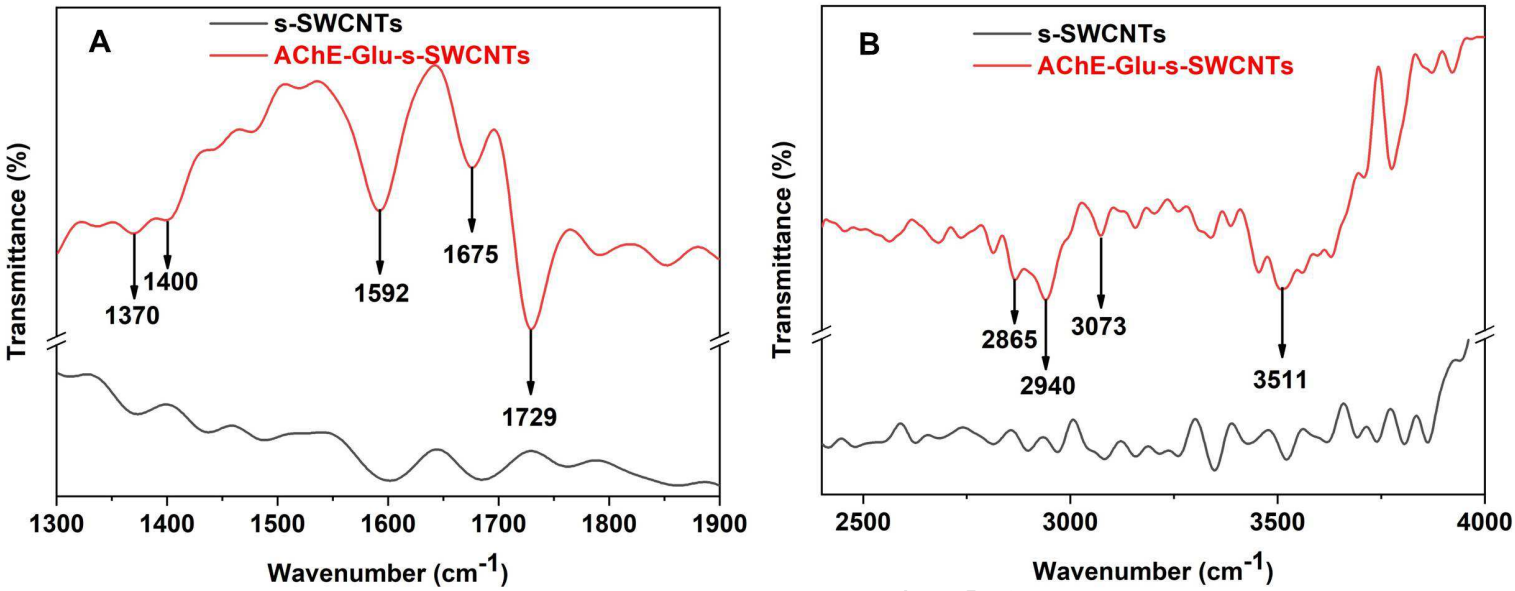

Fig. 2 FT-IR spectra of s-SWCNTs and AChE-Glu-s-SWCNTs films: (A) From 1300 cm^{-1} and 1900 cm^{-1} & (B) From 2400 cm^{-1} and 4000 cm^{-1}.

ACCEPTED MANUSCRIPT

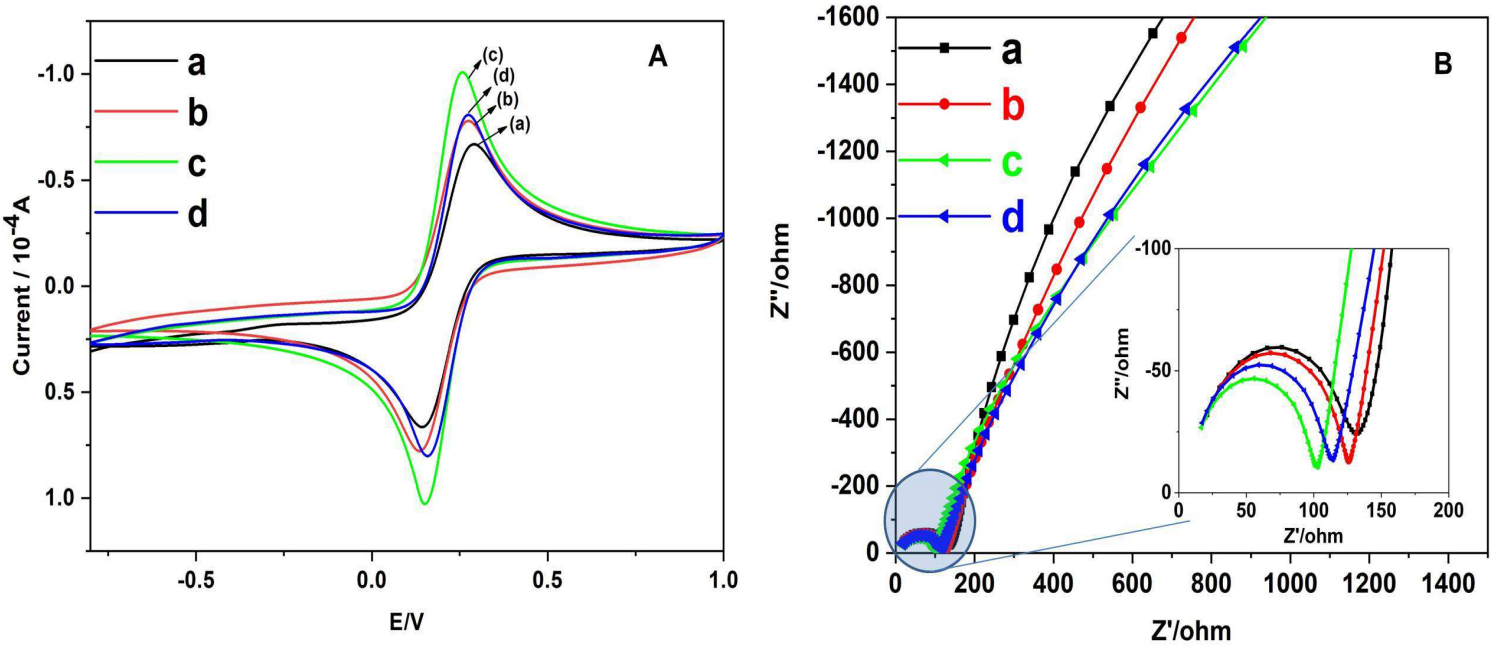

Fig. 3 (A) CVs of (a) bare-GCE, (b) s-SWCNTs/GCE, (c) BSA/AChE-s-SWCNTs/GCE, (d) BSA/AChE-Glu-s-SWCNTs/GCE in 100 mM KCl containing 5 mM $K_3[Fe(CN)_6]$ and 5 mM $K_4[Fe(CN)_6]$. (**B)** EIS Nyquist plots of (a) bare-GCE, (b) s-SWCNTs/GCE, (c) BSA/AChE-s-SWCNTs/GCE and (d) BSA/AChE-Glu-s-SWCNTs/GCE in 100 mM KCl containing 5 mM $K_3[Fe(CN)_6]$ and 5 mM $K_4[Fe(CN)_6]$. EIS measured condition: Amplitude: 50 mV, Frequency: 10 Hz to 1,000,000 Hz, Initial electrode potential: 0 V.

ACCEPTED MANUSCRIPT

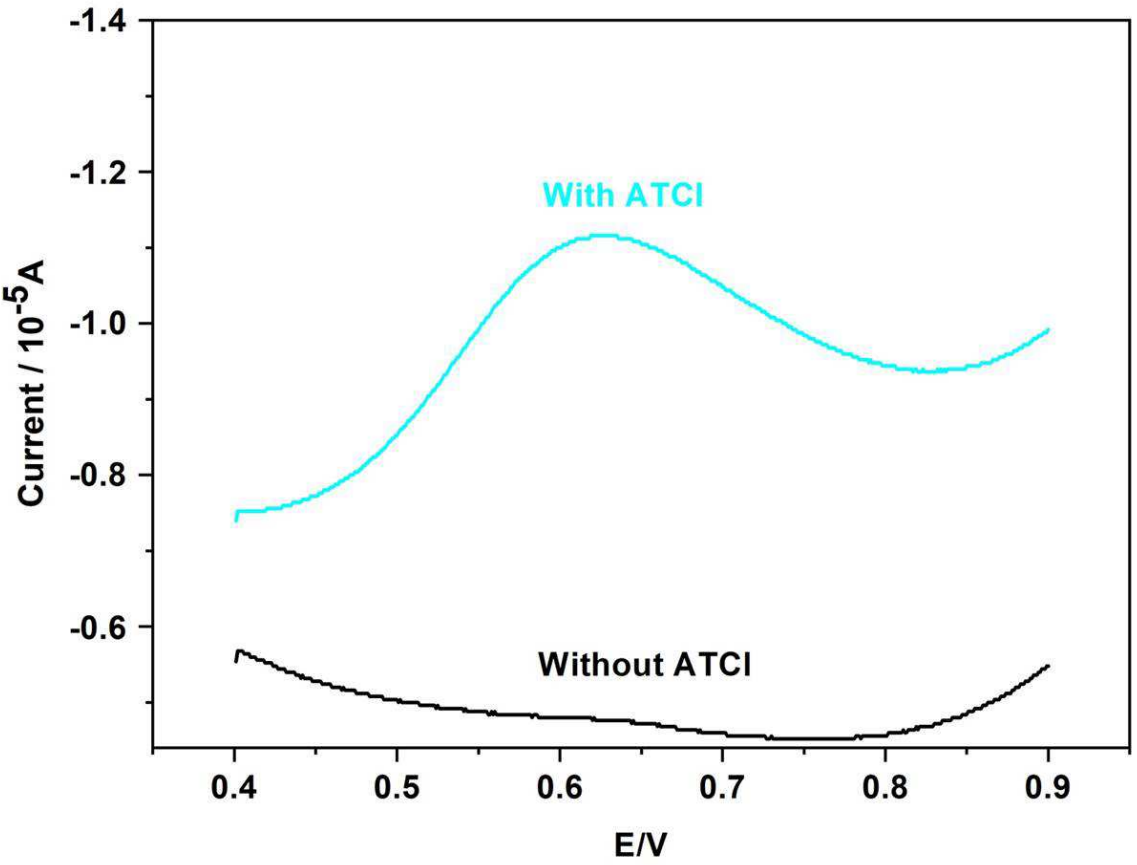

Fig. 4 SWV current responses of the BSA/AChE-Glu-s-SWCNTs/GCE biosensor with and without 4 mM ATCl. SWV measured conditions: SWV frequency 25 HZ, amplitude 100 mV and step potential 1 mV.

ACCEPTED MA

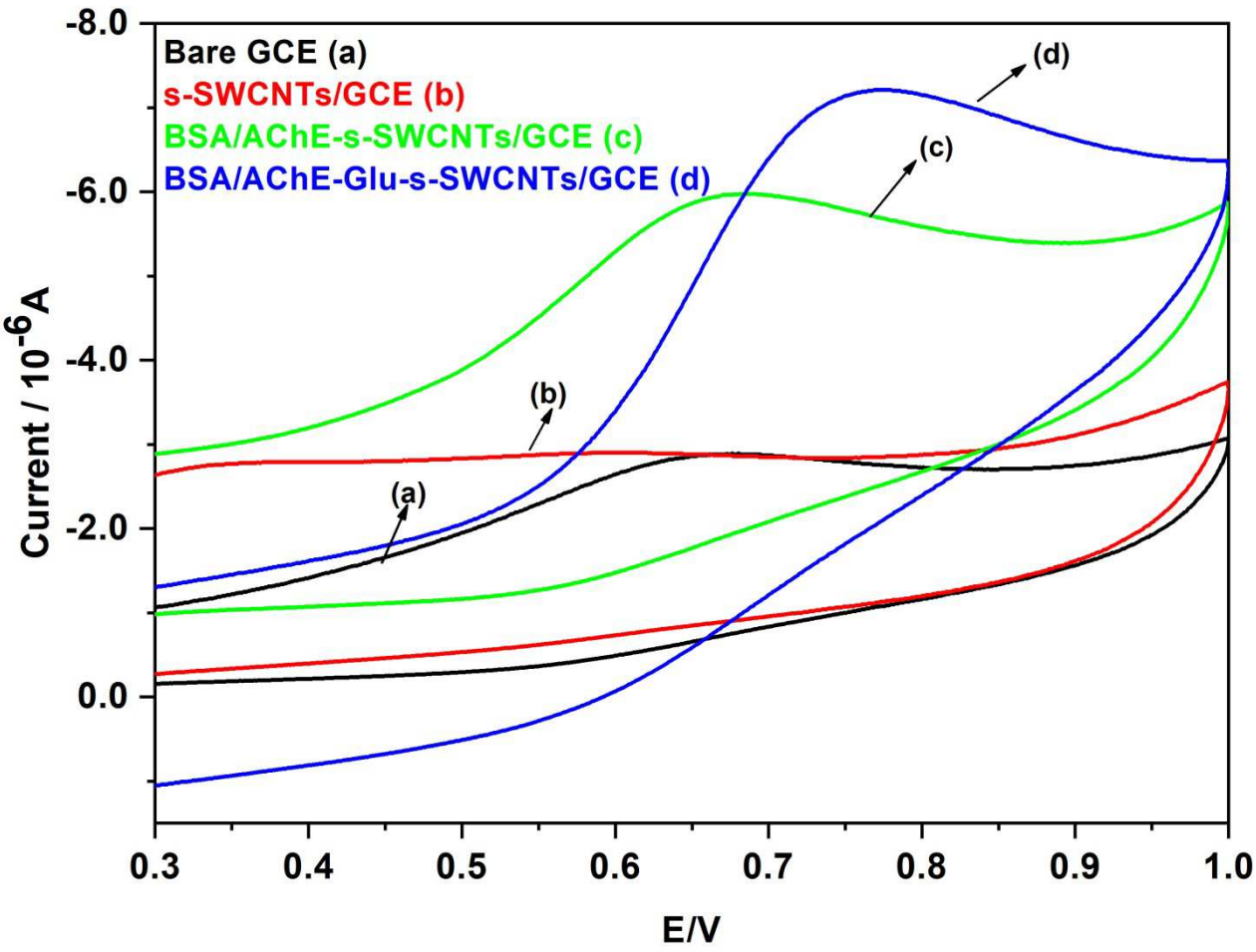

Fig. 5 CVs of (a) Bare GCE, (b) s-SWCNTs/GCE, (c) BSA/AChE-s-SWCNTs/GCE, and (d) BSA/AChE-Glu-s-SWCNTs/GCE in 100 mM PBS (pH 7.4) containing 4 mM ATCl at a scan rate of 100 mV s^{-1}.

ACCEPTED

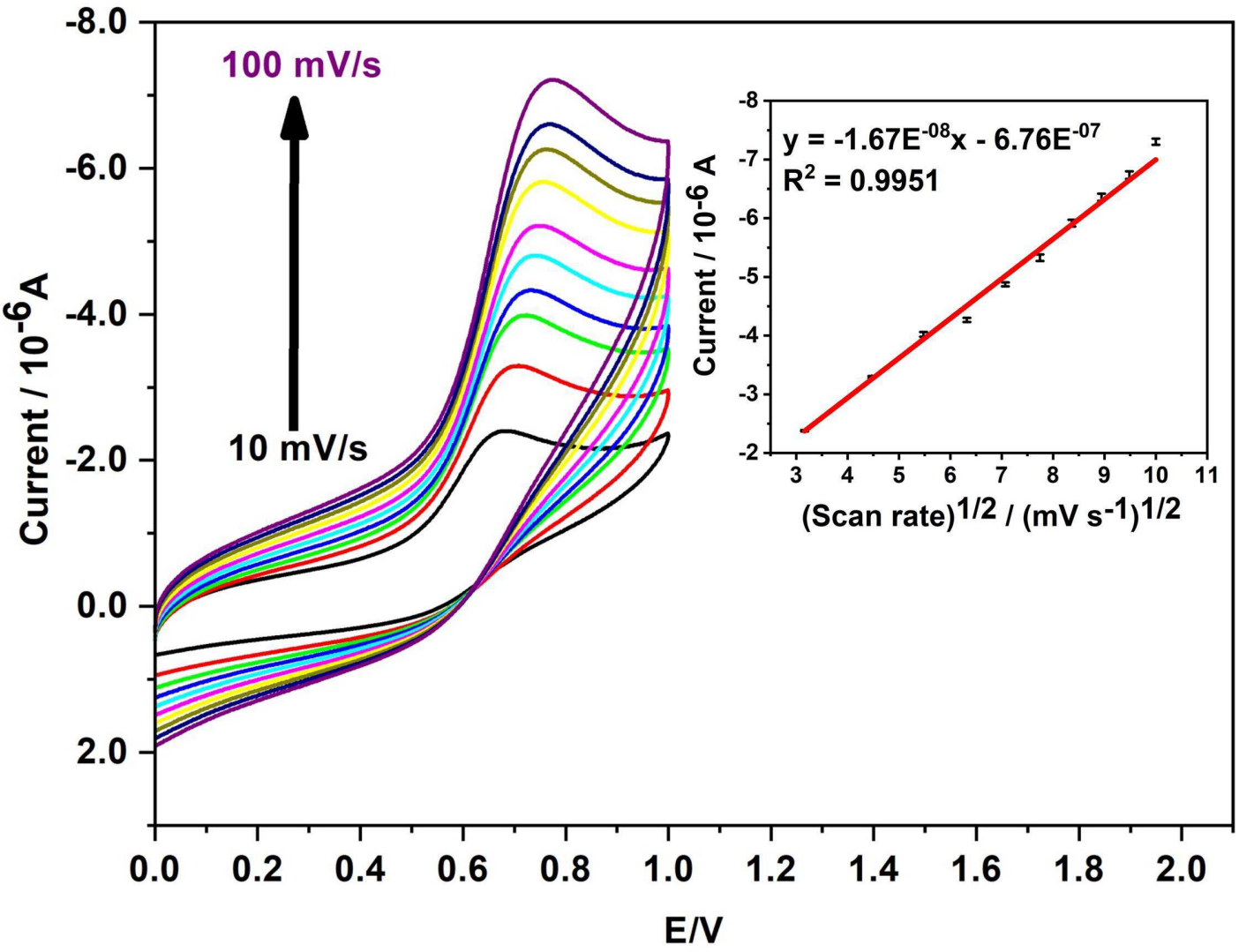

Fig. 6 CVs of BSA/AChE-Glu-s-SWCNTs/GCE in 100 mM PBS (pH 7.4) containing 4 mM ATCl at different scan rates (from 10 to 100 mV s^{-1}). Inset: the plots of the anodic peak currents *vs.* the square root of scan rates (Error bars shows the standard deviation (SD) of three repetitive experiments).

ACCEPTED

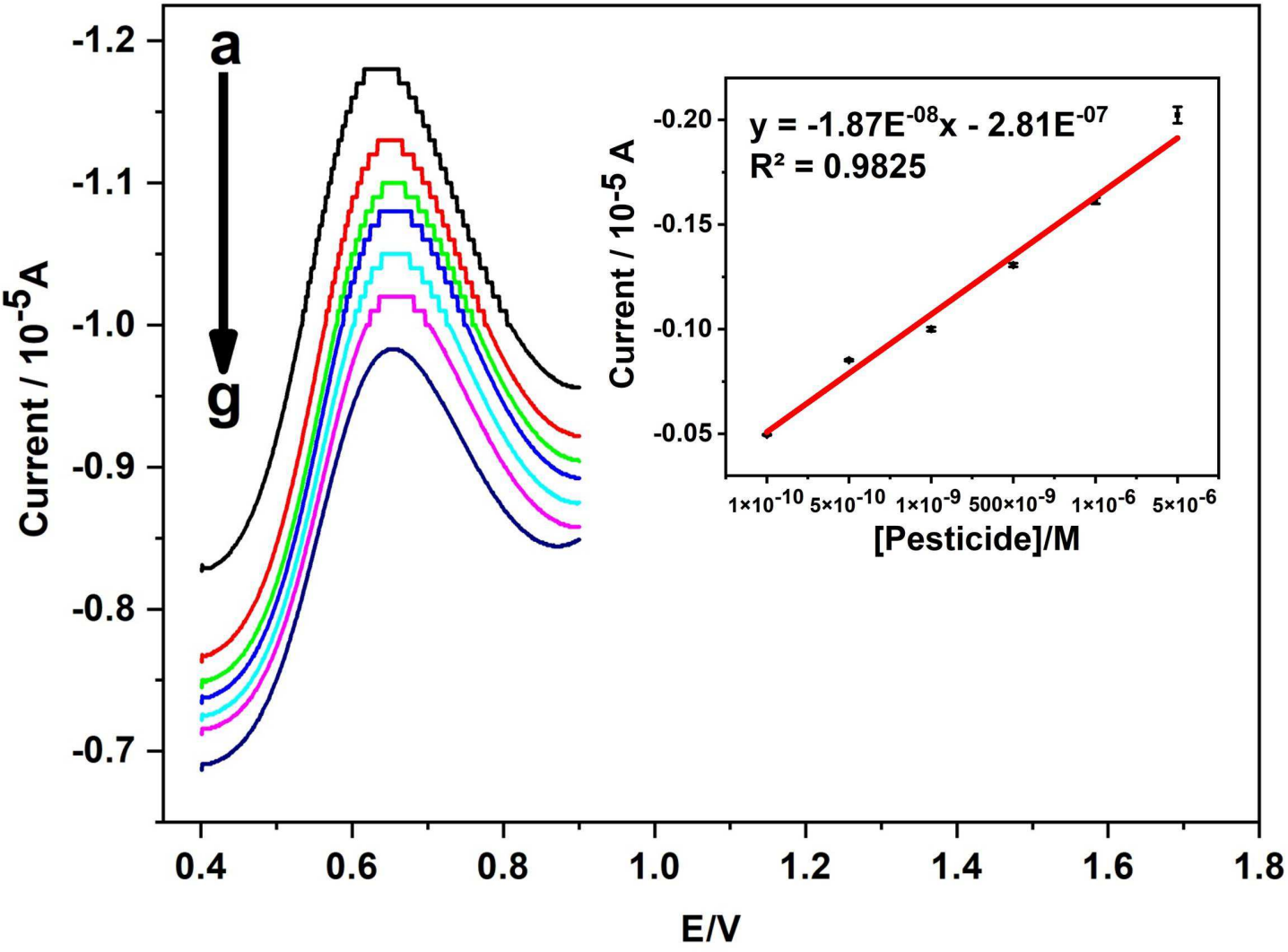

Fig. 7 SWVs of BSA/AChE-Glu-s-SWCNTs/GCE in 100 mM PBS (pH 7.4) containing 4 mM ATCl with different concentration of MP (from a to g): 0, 1×10^{-10} M, 5×10^{-10} M, 1×10^{-9} M, 500×10^{-9} M, 1×10^{-6} M and 5×10^{-6} M. SWV measured condition: Refer **Fig. 4**. Inset: the corresponding calibration plot of MP concentrations against net current responses (Error bars shows the SD of three repetitive experiments).

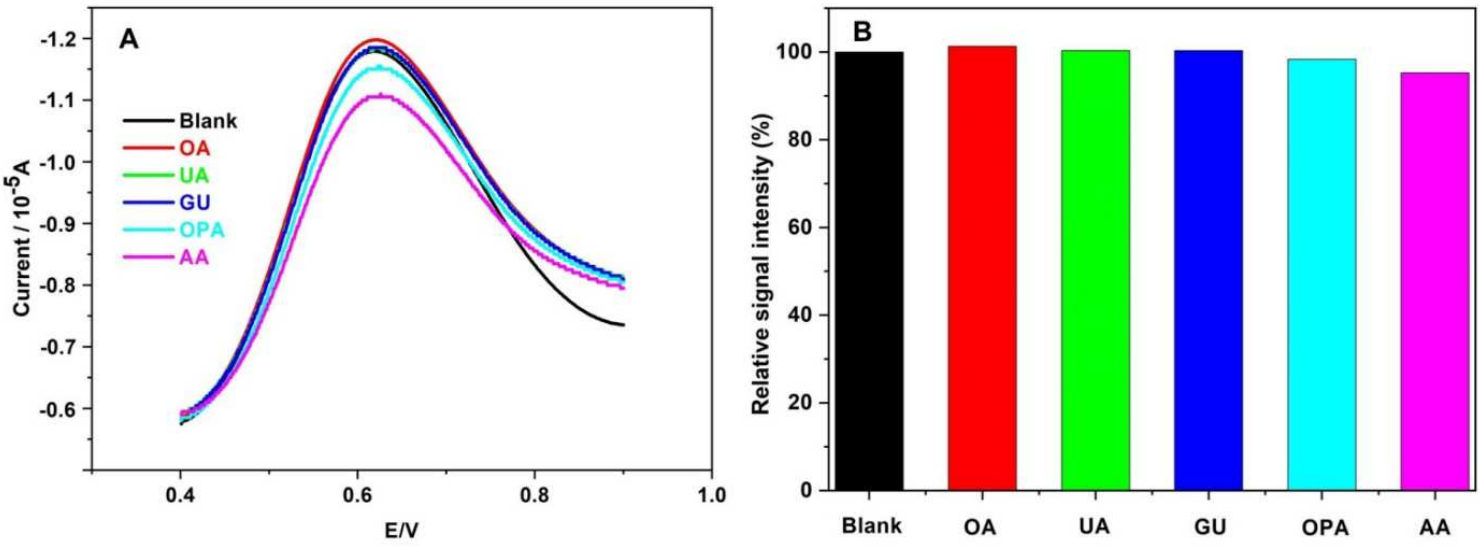

Fig. 8 (A) SWVs of BSA/AChE-Glu-s-SWCNTs/GCE in 100 mM PBS (pH 7.4) containing 4 mM ATCl (blank) and after incubation with 100×10^{-6} M of oxalic acid (OA), uric acid (UA), glucose (GU), orthophosphoric acid (OPA) and ascorbic acid (AA). SWV measured condition: Refer **Fig. 4**. (**B)** Graph demonstrates the changes in biosensors response (relative signal intensity) with different interferent molecules.

ACCEPTED MANUSCRIPT

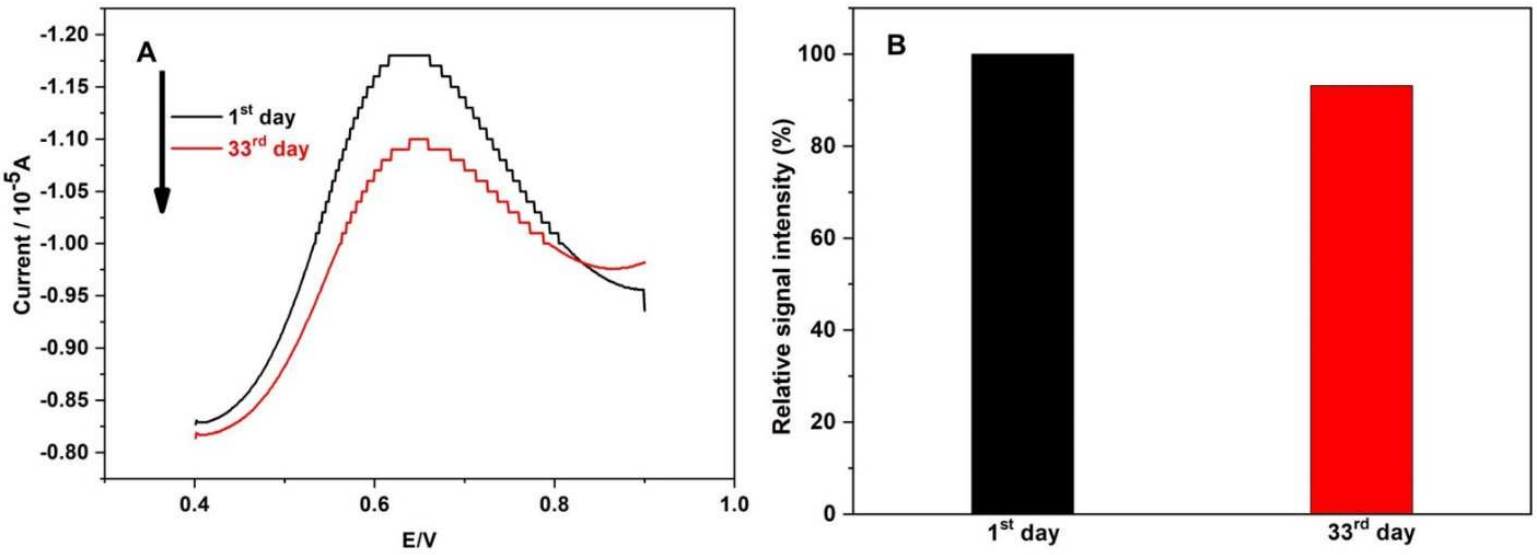

Fig. 9 (A) SWVs of BSA/AChE-Glu-s-SWCNTs/GCE in 100 mM PBS (pH 7.4) containing 4 mM ATCl after several days of storage. SWV measured condition: Refer **Fig. 4**. **(B)** Graph demonstrates the changes in biosensor relative signal intensity with storage period.

ACCEPTED MANUSCRIPT

ACCEPTED MANUSCRIPT

Table 1. Analytical comparison of this new biosensor performance against other reported electrochemical sensors for MP.

Modified electrode	Enzymatic/ Non-Enzymatic	Technique	Electrolyte	Wide linear range (WLR)	Limit of detection (LOD)	References
Ag/GNRs/SPCE	Non-Enzymatic	Amperometry	PBS (pH 7.0)	5×10^{-9} to 2.78×10^{-3} M	0.5×10^{-9} M	[18]
Nano TiO_2/ graphene composite/GCE	Non-Enzymatic	LSV	Acetate buffer (pH 5.2)	2×10^{-9} to 5×10^{-6} M; 5×10^{-6} to 1×10^{-4} M;	1×10^{-9} M	[74]
Graphene/GdHCF/GCE	Non-Enzymatic	DPV	PBS (pH 6.0)	8×10^{-9} to 10×10^{-6} M	1×10^{-9} M	[75]
Ag/NF composite	Non-Enzymatic	Amperometry	B-R buffer (pH 2.56)	0.2×10^{-6} to 1×10^{-6} M	0.2×10^{-6} M	[76]
AChE/LDHs/GCE	Enzymatic	Amperometry	PBS (pH 8.0)	1.9×10^{-8} to 1.5×10^{-5}	2.3×10^{-9} M	[45]
Au/ssDNA-SWCNT/PANI-AChE/GCE	Enzymatic	SWV	PBS (pH 7.0)	1×10^{-11} to 1×10^{-6} M	1×10^{-12} M	[48]
AChE/SF/MWNTs/GCE	Enzymatic	Amperometry	PBS (pH 7.0)	3.5×10^{-6} to 2×10^{-3}	5×10^{-7} M	[46]
NF/AChE-CS/Pt NPs/CGR-NF/GCE	Enzymatic	CV	PBS (pH 7.4)	10^{-13} to 10^{-10} ; 10^{-10} to 10^{-8}	5×10^{-14} M	[77]
NF/AChE-CS/NiO-CGR-NF/GCE	Enzymatic	CV	PBS (pH 7.4)	10^{-13} to 10^{-10} ; 10^{-10} to 10^{-8}	5×10^{-14} M	[47]
BSA/AChE-Glu-s-SWCNTs/GCE	Enzymatic	SWV	PBS (pH 7.4)	1×10^{-10} M to 5×10^{-6} M	3.75×10^{-11}M	This work

Au : gold; ssDNA : single strand oligonucleotide; PANI : polyaniline; Ag : silver; GNR : graphene nanoribbons; SPCE : screen printed carbon electrode; LSV : linear sweep voltammetry; GdHCF : gadolinium hexacyanoferrate nanocomposite; B-R buffer : britton-robinson buffer; DPV : differential pulse voltammetry; LDHs : layered double hydroxides; SF : silk fibroin; CS : chitosan; NF : nafion; Pt NPs : platinum nanoparticles; CGR : carboxylic graphene; CV : cyclic voltammetry; NiO : nickel oxide; TiO_2 : titanium dioxide.

ACCEPTED MANUSCRIPT

Highlights

- A simple electrochemical biosensor is reported for methyl parathion (MP) pesticide detection in fruits samples using high purity s-SWCNTs modified electrode.
- The fabricated biosensor was characterized by CV, FT-IR, TEM, EIS and SWV.
- The proposed BSA/AChE-Glu-s-SWCNTs/GCE biosensor exhibited a wide linear range from 1×10^{-10} M to 5×10^{-6} M with LOD of 3.75×10^{-11} M for MP target.
- The BSA/AChE-Glu-s-SWCNTs/GCE biosensor showed high selectivity and stability.
- The RSD of the proposed BSA/AChE-Glu-s-SWCNTs/GCE biosensor was calculated to be 0.89% and recovery was 99.03% for MP target.

ACCEPTED MANUSCRIPT